

Density of states of a dissipative quantum dot coupled to a quantum wire

Moshe Goldstein and Richard Berkovits

The Minerva Center, Department of Physics, Bar-Ilan University, Ramat-Gan 52900, Israel

We examine the local density of states of an impurity level or a quantum dot coupled to a fractional quantum Hall edge, or to the end of a single one-dimensional Luttinger-liquid lead. Effects of an Ohmic dissipative bath are also taken into account. Using both analytical and numerical techniques we show that, in general, the density of states exhibits power-law frequency dependence near the Fermi energy. In a substantial region of the parameter space it simply reflects the behavior of the tunneling density of states at the end of a Luttinger-liquid, and is insensitive either to the value of the dot-lead interaction or to the strength of dissipation; otherwise it depends on these couplings too. This behavior should be contrasted with the thermodynamic properties of the level, in particular, its occupancy, which were previously shown to depend on the various interactions in the system only through the corresponding Fermi edge singularity exponent, and thus cannot display any Luttinger-liquid specific power-law. Hence, we can construct different models, some with and some without interactions in the wire (but with equal Fermi edge singularity exponents), which would have very different level densities of states, although they all result in the same level population vs. energy curves.

PACS numbers: 73.23.Hk, 71.10.Pm, 73.20.Hb

I. INTRODUCTION

Understanding the behavior of low-dimensional electronic systems has been one of the main challenges of experimental and theoretical physics in the last years. These systems are important not only as the basic building blocks of nanoelectronic devices, but also for the intricate strongly-correlated phenomena they exhibit. An important subclass is that of metallic (gapless) one-dimensional systems, whose low energy dynamics is governed not by Fermi liquid theory, but instead by the Luttinger liquid (LL) paradigm¹. This description applies to a wide variety of experimental realizations, including narrow quantum wires in semiconducting heterostructures, metallic nanowires, and carbon nanotubes. Closely related are chiral LLs, formed at the edges of fractional quantum Hall effect (FQHE) systems², and helical LLs, the edges of spin quantum Hall insulators³. The effect of impurities on these systems is interesting from both the applicative and fundamental points of view. These impurities could also be intentionally introduced, in the form of, e.g., quantum dots and anti-dots. Hence, there is no wonder that such questions have attracted much effort recently. However, most of these studies were restricted to investigation of transport phenomena^{1–13}, while other effects received much less attention^{14–22}.

In this work we study probably the most basic example of such a system, namely, a single level in the vicinity of a fractional quantum Hall edge, or, equivalently²³, a level attached to the end of a single LL wire¹⁴. We will refer to the two components (in both systems) as “dot” and “lead” respectively. We include in our treatment the effects of short range dot-lead interaction, as well as the influence of an Ohmic dissipative bath (e.g., electromagnetic fluctuations in gate electrodes)^{16,24–26}. In a recent work²¹ we have studied the thermodynamic properties of the model (e.g., the level population, entropy,

and specific heat), and found that they are *universal*, in the sense that they depend on the various interactions in the model (intra-lead, dot-lead, and dot-bath) only through a single parameter, the Fermi edge singularity exponent. Thus, thermodynamics can neither be used to identify non-Fermi liquid behavior, nor to extract LL parameters. In this work we proceed to study, both analytically and numerically, the level density of states (LDoS), which may be probed by tunneling or absorption spectroscopies. We find that the LDoS is sensitive to LL physics, even though its integral (times the Fermi function) gives the level occupancy, which is universal in the above sense. As we show below, the LDoS features power-law behavior near the Fermi energy. For not too strong interactions the exponent in this power-law is actually determined by LL physics alone, and is independent of the level-lead and level-bath interactions. This and many other results derived below cannot be achieved using perturbative calculations¹⁹.

The rest of this paper is organized as follows: In Sec. II we present our model, and apply to it the Anderson-Yuval Coulomb-gas (CG) expansion^{26–31}. We then proceed to analytic treatment of the LDoS in Sec. III, and to numerical calculations in Sec. IV. Finally, we summarize our findings in Sec. V.

II. MODEL AND COULOMB-GAS EXPANSION

The system is described by the Hamiltonian $H = H_D + H_L + H_{DL} + H_B + H_{DB}$. The first term is the dot Hamiltonian $H_D = \varepsilon_0 d^\dagger d$, with d^\dagger and d the level creation and annihilation operators, respectively, and ε_0 the level energy. The second term is the lead Hamilto-

nian. It can be written in the form

$$H_L = \frac{v}{4\pi} \int_{-\infty}^{\infty} [\partial_x \phi(x)]^2 dx, \quad (1)$$

using *chiral* bosonic field $\phi(x)$ obeying the commutation relation $[\phi(x), \phi(y)] = i\pi \text{sgn}(x-y)$, where v is the velocity of excitations²³. The level and the lead are coupled by:

$$H_{DL} = t_0 d^\dagger \psi(0) + \text{H.c.} + U_0 \left(d^\dagger d - \frac{1}{2} \right) \frac{\sqrt{g}}{\pi} \partial_x \phi(0). \quad (2)$$

The two terms in this equation describe, respectively, dot-lead hopping (with t_0 the tunneling matrix element), and local dot-lead interaction whose strength is U_0 . The electronic annihilation operator at the end of the lead can be written as $\psi(0) = \chi e^{i\phi(0)/\sqrt{g}}/\sqrt{2\pi a}$, where χ is a Majorana operator, a is a short distance cutoff (e.g., the lattice spacing), and g is the LL interaction parameter ($g < 1$ for repulsion, $g > 1$ for attraction). For a FQHE system with filling ν , $g = \nu$ for electron tunneling (i.e., a dot outside the FQHE bar). Finally, the level is coupled to a bath of harmonic oscillators^{16,24–26} (describing, e.g., electromagnetic fluctuations in control gates), governed by $H_B = \sum_k \omega_k a_k^\dagger a_k$. The dot-bath coupling can be written as $H_{DB} = (d^\dagger d - \frac{1}{2}) \sum_k \lambda_k (a_k^\dagger + a_k)$. We assume Ohmic dissipation, i.e., linear low-frequency behavior of the bath spectral function: $J_B(\omega) \equiv \sum_k \lambda_k^2 \delta(\omega - \omega_k) = K\omega$.

We examine this model employing the Anderson-Yuval CG expansion²⁷. In this approach, any quantity of interest is expanded to all orders in t_0 . This results in a series of correlation functions, which need to be evaluated for vanishing t_0 .^{26–31} The level-lead interaction gives rise to a potential at the end of the lead, which alternates between $U_0/2$ and $-U_0/2$ whenever an electron tunnels in or out of the level. Similarly, the k th bath oscillators experience a shift in its equilibrium position, proportional to λ_k . We thus have a sequence of Fermi edge singularity events³². The solution of this latter problem enables the calculation of all the terms in the series of correlation functions.

Recently²¹ we have studied in this way the partition function Z of the model, whose derivatives with respect to the parameters of the system (for example, the level energy ε_0 and the temperature T) give us the thermodynamic properties (e.g., the level population, entropy, and specific heat). We were able to rewrite the series expansion for Z in the form of a grand canonical partition function of a classical system of particles. These represent hopping events generated by t_0 , and thus reside on the imaginary time axis of the original quantum model, which is a circle with circumference $1/T$. Each particle is assigned a positive (negative) charge if it represents tunneling of an electron from the lead to the dot (from the dot to the lead). Hence, there must be an even number of charges, which have to appear in alternating order of

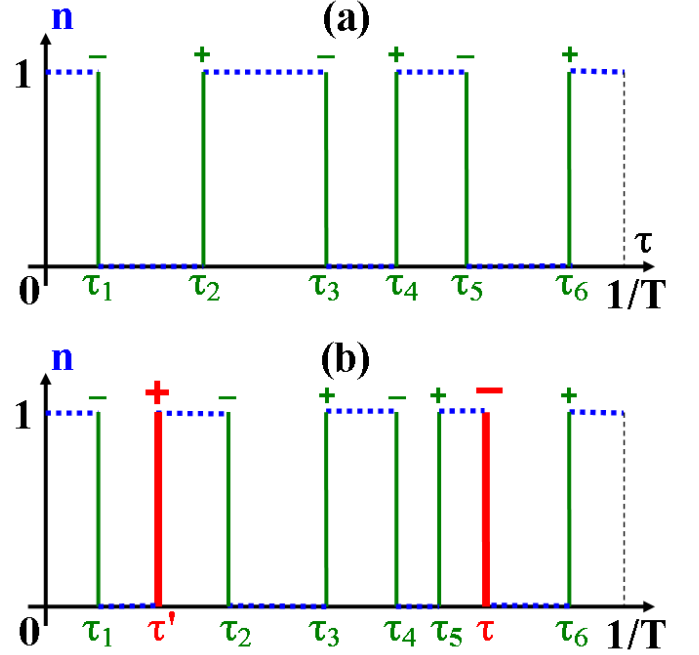


FIG. 1: (Color online) A typical term (with $2N = 6$ t_0 -charges and $s = -1$) in the CG expansions for (a) the partition function [Eqs. (3)–(4)]; (b) the dot Green function for $\tau > \tau'$ [Eqs. (5)–(6)] (here $s' = 1$ and $M = 0$ so a single t_0 -charge precedes τ' , whereas there are $2M' = 4$ t_0 -charges between τ' and τ). Signs and positions of the charges are indicated, with t_0 -charges marked by thin green vertical lines, and d-charges by wide red ones. Level population as function of imaginary time is denoted by horizontal dashed blue lines.

signs. The position of the i th particle is τ_i , and the sign of the charge of the first particle is denoted by s . The partition function then reads:

$$Z = \sum_{\substack{N=0 \\ s=\pm 1}}^{\infty} y^{2N} \int_0^{1/T} \frac{d\tau_{2N}}{\xi} \int_0^{\tau_{2N}-\xi} \frac{d\tau_{2N-1}}{\xi} \dots \int_0^{\tau_3-\xi} \frac{d\tau_2}{\xi} \int_0^{\tau_2-\xi} \frac{d\tau_1}{\xi} e^{-S_{CG}(s, \{\tau_i\})}, \quad (3)$$

The charges have a fugacity $y = \sqrt{\Gamma_0 \xi / \pi}$, where $\Gamma_0 = \pi |t_0|^2 \rho_L$ is the noninteracting level width [$\rho_L = 1/(\pi v)$ is the corresponding lead local density of states], and $\xi \sim a/v$ is a short-time cutoff. The CG action is given by:

$$S_{CG}(s, \{\tau_i\}) = \sum_{i < j=1}^{2N} \vec{e}_i \cdot \vec{e}_j V_C(\tau_j - \tau_i) + \varepsilon_0 \left[\frac{1-s}{2T} + s \sum_{i=1}^{2N} (-1)^i \tau_i \right]. \quad (4)$$

The first term of this classical Hamiltonian describes an interaction between the particles, with $V_C(\tilde{\tau}) = \ln\{\pi T\xi/\sin[\pi T|\tilde{\tau}|\}\}$. This interaction is similar in form to 2D Coulomb interaction, and is the origin of the name “CG expansion”. The charges are two component vectors, where the two components correspond to the effects of the coupling with the lead and the bath, respectively. They are given by $\vec{e}_i = s(-1)^{i-1}\vec{e}_0$, where the squared-magnitude of the charges, to be denoted by $\alpha_{\text{FES}} \equiv |\vec{e}_0|^2$, is the Fermi edge singularity exponent of the model. It is defined by behavior of the zero-temperature correlator of $d^\dagger\psi(0)$ with its Hermitian conjugate, calculated at $t_0 = 0$. This correlator decays as $\tilde{\tau}^{-\alpha_{\text{FES}}}$ for long time $\tilde{\tau}$. In our system we have found that $\vec{e}_0 = (1/\sqrt{g} - 2\sqrt{g}\delta_{\text{eff}}/\pi, \sqrt{K})$, where δ_{eff} is the effective phase shift in the lead due to the dot-lead coupling²¹. It is equal to $U_0/(2v)$ in straightforward bosonization, but is more complicated in general. It may be extracted from, e.g., finite-size energy differences, which could be calculated either numerically or analytically (via the Bethe ansatz)²¹. The other part of the CG action accounts for the energetic cost of ε_0 per unit imaginary time for each interval in which the level is populated. Its form is analogous to an electric field applied to the classical system of

charges. A typical configuration is depicted in Fig. 1(a).

A similar treatment can be given to the LDoS, which we shall denote by $\rho_D(\omega)$. It is equal to the imaginary part of the level retarded Green function (multiplied by $-1/\pi$). The retarded Green function is in turn the result of analytic continuation of the Matsubara Green function from the upper half of the complex frequency plane³³. The latter Green function is defined by $G_D(\tau - \tau') = -\text{Tr}\{\hat{T}_\tau e^{-H/T} d(\tau) d^\dagger(\tau')\}/Z$, where \hat{T}_τ is the imaginary time ordering operator. Following the same methods as above, the numerator of this expression can also be given a CG representation. This CG has the same form as Eqs. (3)–(4), with two additional charges of sizes $\pm\vec{e}_d$, $\vec{e}_d = \vec{e}_0 - (1/\sqrt{g}, 0)$, inserted at τ' and τ , respectively. These charges correspond to the level creation and annihilation operators appearing in the definition of the Green function. In the following we will refer to these as “d-charges”, to distinguish them from the other “ t_0 -charges”, which originate from the t_0 term. The contribution of each such configuration is to be multiplied by $\text{sgn}(\tau' - \tau)$ to account for the Fermi statistics. Thus, for $\tau > \tau'$ the full CG expression for the dot Green function is:

$$G_D(\tau > \tau') = -\frac{1}{Z} \sum_{\substack{N=0 \\ s=\pm 1}}^{\infty} y^{2N} \sum_{M=0}^{N-s'} \sum_{M'=0}^{N-s'-M} \int_{\tau+\xi}^{1/T} \frac{d\tau_{2N}}{\xi} \dots \int_{\tau+\xi}^{\tau_{2(M+M')+\tau'+2-\xi}} \frac{d\tau_{2(M+M')+\tau'+1}}{\xi} \times \\ \int_{\tau'+\xi}^{\tau-\xi} \frac{d\tau_{2(M+M')+\tau'}}{\xi} \dots \int_{\tau'+\xi}^{\tau_{2M+\tau'+2-\xi}} \frac{d\tau_{2M+\tau'+1}}{\xi} \int_0^{\tau'-\xi} \frac{d\tau_{2M+\tau'}}{\xi} \dots \int_0^{\tau_1-\xi} \frac{d\tau_1}{\xi} e^{-S_{CG,D}(s,\tau,\tau',\{\tau_i\})}, \quad (5)$$

where $s' \equiv (1-s)/2$. The first $2M + s'$ t_0 -charges occupy the interval $[0, \tau']$, the following $2M'$ charges reside in the interval $[\tau', \tau]$, and the last $2(N - M - M') - s'$ t_0 -charges are in the interval $[\tau, 1/T]$. The classical action is given by:

$$S_{CG,D}(s,\tau,\tau',\{\tau_i\}) = |\vec{e}_0|^2 \sum_{i<j=1}^{2N} s_i s_j V_C(\tau_j - \tau_i) + \vec{e}_0 \cdot \vec{e}_d \sum_{i=1}^{2N} s_i [V_C(\tau_i - \tau') - V_C(\tau_i - \tau)] - |\vec{e}_d|^2 V_C(\tau - \tau') + \\ \varepsilon_0 \left[\frac{1-s}{2T} - \sum_{i=1}^{2N} s_i \tau_i + \tau - \tau' \right], \quad (6)$$

where the sign of the i th t_0 -charge is $s_i = s(-1)^{i-1} \text{sgn}(\tau_i - \tau') \text{sgn}(\tau_i - \tau)$. A typical configuration is shown in Fig. 1(b). Similar expressions hold for $\tau < \tau'$.

Comparing the two CG expansions, the following observation emerges: the CG expansion for the partition function contains only three parameters: Γ_0 , ε_0 , and α_{FES} , while expansion for the Green function depends on g too (through \vec{e}_d). Hence, the different interaction

types (i.e., interactions in the wire, the dot-wire interaction, and the dot-bath coupling) affect the partition function through a single parameter, the Fermi edge singularity exponent α_{FES} . Thus, thermodynamic measurements cannot be used to distinguish between the different interaction types. In other words, one can construct very different models, whose interactions differ in strength and even in sign, which will have the same thermodynamic

properties, provided Γ_0 , ε_0 , and α_{FES} are indeed the same²¹. On the other hand, the LDoS, which depends *explicitly* on g , will exhibit different behavior for these different systems. Hence, it can be used to extract the strength of intra-wire interactions, as we show below.

III. ANALYSIS OF THE LEVEL DENSITY OF STATES

As noted in our earlier work²¹, the CG obtained here is identical to the original Anderson-Yuval expansion²⁷ for the anisotropic single-channel Kondo model³⁴, demonstrating that the models are equivalent^{14,16}. Under this mapping the level population becomes the magnetization of the Kondo spin (plus one half). Hence, ε_0 is analogous to a local magnetic field. Similarly, J_{xy} is related to Γ_0 , and J_z to α_{FES} . The CG parameters obey the famous Kondo renormalization group (RG) equations^{27,34}, which read, in our notations:

$$\frac{dy}{d \ln \xi} = \frac{2 - \alpha_{\text{FES}}}{2} y, \quad (7)$$

$$\frac{d\alpha_{\text{FES}}}{d \ln \xi} = -4y^2 \alpha_{\text{FES}}. \quad (8)$$

Thus, the system considered can be in one of two phases, a strong coupling (antiferromagnetic-Kondo like) phase and a weak coupling (ferromagnetic-Kondo like) phase. The transition occurs, for small Γ_0 , at $\alpha_{\text{FES}} = 2 + O(\sqrt{\Gamma_0 a/v})$. In the weak-coupling phase the Coulomb charges form tightly-bound pairs. The level is thus effectively decoupled at low energies, resulting in its population being discontinuous as a function of ε_0 at zero temperature^{14,16,18}. In the strong-coupling phase free Coulomb charges proliferate. The impurity is well-coupled with the lead, so the level population is analytic in ε_0 , and could be extracted from the Bethe ansatz solution of the Kondo problem³⁴. In particular, for small values of ε_0 one has $n(\varepsilon_0) - 1/2 \sim -\varepsilon_0/T_K$, where $T_K = (v/a)(\Gamma_0 a/v)^{1/(2-\alpha_{\text{FES}})}$ is the Kondo temperature (effective level width, reducing to Γ_0 in the noninteracting case)¹⁹. Hence, in this phase the population does not exhibit any nontrivial power-law dependence on ε_0 or T . The same applies to other thermodynamic quantities.

What are the implications of this on the LDoS? As we now show, we typically find that at zero temperature we have a power-law behavior $\rho_D(\omega) \sim |\omega|^\delta$ in the vicinity of the Fermi energy, i.e., when $|\omega|$ is much smaller than T_K in the strong-coupling phase, and than the bandwidth $\sim v/a$ in the weak-coupling phase. The values of δ in the different regimes are summarized in Table I. It should be noted that when $T > 0$, or when the lead length L is finite, such power-law singularity will be smeared and become $[\max(|\omega|, T, v/L)]^\delta$. We will now consider each phase separately.

TABLE I: Summary of the analysis of Sec. III. In the vicinity of the Fermi energy (when $|\omega|$ and T are much smaller than T_K in the strong-coupling phase, and than the bandwidth $\sim v/a$ in the weak-coupling phase) we have $\rho_D(\omega) \sim [\max(T, |\omega|)]^\delta$, with the values of the exponent δ in the different regimes denoted in the table below. When two values are given, the smaller one will give the dominant contribution³⁵.

Phase	$ \omega \ll \varepsilon_0 $	$ \omega \gg \varepsilon_0 $
Strong-coupling	$1/g - 1$	$1/g - 1$
Weak-coupling	$1/g - 1$	$\alpha_{\text{FES}}^d - 1$ or $1/g - 1$

A. The strong-coupling phase

Let us start from the strong-coupling phase. When $|\varepsilon_0|$ is large enough (with respect to T_K), CG charges must appear in tightly-bound pairs, since large intra-pair separation is suppressed by the level energy, as dictated by the last term of Eq. (6). The two d-charges added in the calculation of the level Green function will also be accompanied by two screening t_0 -charges for the same reason. The resulting configuration should thus resemble Fig. 2(a). The leading contribution to the Green function will then come from the residual interaction of these partially screened d-charges, whose charges are (± 1 times) $\vec{e}_0 - \vec{e}_d = (1/\sqrt{g}, 0)$. Thus, for large $\tau - \tau'$ we have $G_D(\tau - \tau') \sim \text{sgn}(\tau' - \tau)|\tau - \tau'|^{-1/g}$. This leads to $\rho_D(\omega) \sim |\omega|^{1/g-1}$, the usual tunneling density of states singularity at the end of a LL wire^{1,4}.

When ε_0 is small (with respect to T_K), renormalization effects are significant. In addition to the usual CG RG Eq. (8) representing the screening of interaction between t_0 -charges by pairs of nearby t_0 -charges (separated by ξ)²⁷, one can write down similar equations for the flow of the Green function parameters³⁰. It is easy to see that the coefficients of the logarithmic interaction between any two charges (either both t_0 -charges, both d-charges, or a mixed pair) are renormalized in the same way by the pairs of nearby t_0 -charges, i.e.,

$$\frac{d(\vec{e}_\mu \cdot \vec{e}_\nu)}{d \ln \xi} = -2y^2 (\vec{e}_\mu \cdot \vec{e}_0 + \vec{e}_0 \cdot \vec{e}_\nu), \quad (9)$$

where $\mu, \nu = 0, d$. Thus, the combination $|\vec{e}_0 - \vec{e}_d|^2 = |\vec{e}_0|^2 + |\vec{e}_d|^2 - 2\vec{e}_0 \cdot \vec{e}_d$ is invariant, and retains its initial value of $1/g$. At the strong coupling fixed point y is large, so, by Eq. (8), $|\vec{e}_d^*| = \sqrt{\alpha_{\text{FES}}^*} = 0$, where asterisks denote fixed-point values. Thus, $|\vec{e}_0^*| = 1/\sqrt{g}$, so that $G_D(\tau' - \tau) \sim (\tau' - \tau)^{-|\vec{e}_d^*|^2} = (\tau' - \tau)^{-1/g}$, resulting again in $\rho_D(\omega) \sim |\omega|^{1/g-1}$. Since this behavior holds at both large and small ε_0 values, it should also apply at all intermediate values.

Further support for this result is obtained by analysis of the particular case $\alpha_{\text{FES}} = 1$ (the Toulouse limit²⁷), where the CG, and all thermodynamic properties, reduce to those of a noninteracting resonant level (for which $g = 1$, $U_0 = 0$, and $K = 0$). A nontrivial (i.e., in-

interacting) realization of this condition, which still permits an exact calculation of the LDoS, is the case of no coupling to a bath ($K = 0$), but with $g = 1/4$ and a corresponding compensating value of the dot-lead interaction. Then $\vec{e}_d = (-1, 0) = -\vec{e}_0$, so the d-charges have the same magnitudes as the corresponding t_0 -charges, but the opposite signs. Comparison of the corresponding CG expansions thus shows that the level Green function of the interacting system is equal to a two-particle Green function of the noninteracting resonant level $\langle \hat{T}_\tau \psi(0, \tau) d(\tau) d^\dagger(\tau') \psi^\dagger(0, \tau') \rangle$, up to a factor of $(2\pi a)^{-1} \text{sgn}(\tau' - \tau)$. The operators at τ and τ' in this noninteracting two-particle Green function are similar to the t_0 term in the Hamiltonian, but with $\psi(0)$ replaced by $\psi^\dagger(0)$ to account for the signs of the d-charges in the interacting system. After a straightforward evaluation of this two particle Green function by Wick's theorem, we find for the LDoS the following expression:

$$\rho_D(\omega) = 2\rho_L a \coth\left(\frac{\omega}{2T}\right) \text{Im} \left\{ \frac{\omega - 2\varepsilon_0 + 2i\Gamma_0}{\omega - 2\varepsilon_0} \times \left[\psi\left(\frac{1}{2} - \frac{\varepsilon_0 - i\Gamma_0}{2\pi iT}\right) - \psi\left(\frac{1}{2} + \frac{\omega - \varepsilon_0 + i\Gamma_0}{2\pi iT}\right) \right] \right\}, \quad (10)$$

where $\psi(z)$ is the digamma function³⁶. For small $|\omega|$ and T we indeed recover the $[\max(T, |\omega|)]^3$ behavior appropriate for $g = 1/4$, for *all* values of ε_0 .

Physically, the result is clear: in the strongly-coupled phase the level behaves, at low energies, as the last site of the lead, so its LDoS is similar to the local density of states near the end of a LL wire^{1,4}, i.e., $\rho_D(\omega) \sim |\omega|^{1/g-1}$. Interestingly, not only dot-lead interactions, but even coupling to the bath does not modify this behavior. As a result of this, the LDoS exhibits a power-law behavior with exponent which depends only on the LL parameter g and not on α_{FES} , i.e., on the interactions in the wire but not on the level-lead and level-bath couplings. This is in contrast with, e.g., the level occupancy, which depends on α_{FES} but not on g , as discussed above. Below we also test these predictions numerically.

B. The weak-coupling phase

We now turn our attention to the weak-coupling phase. Here all the t_0 -charges are bound in pairs, so the high $|\varepsilon_0|$ results discussed above (which should also hold in this phase) actually carry over to low values of $|\varepsilon_0|$. It should however be remembered that then they compete with the contribution of the $t_0 = 0$ term in the CG expansion (the weak coupling fixed point), the term representing the interaction of the unscreened d-charges, which gives the LDoS a contribution of the form $\rho_{\text{pair}}(\omega) \sim |\omega|^{\alpha_{\text{FES}}^d - 1}$, with $\alpha_{\text{FES}}^d \equiv |\vec{e}_d|^2$. This is simply the LDoS of a tunnel-decoupled level, broadened from a delta peak to a power-law by the Anderson orthogonalities in the wire³² and in the Ohmic bath^{24,25}. Note that since the level is effec-

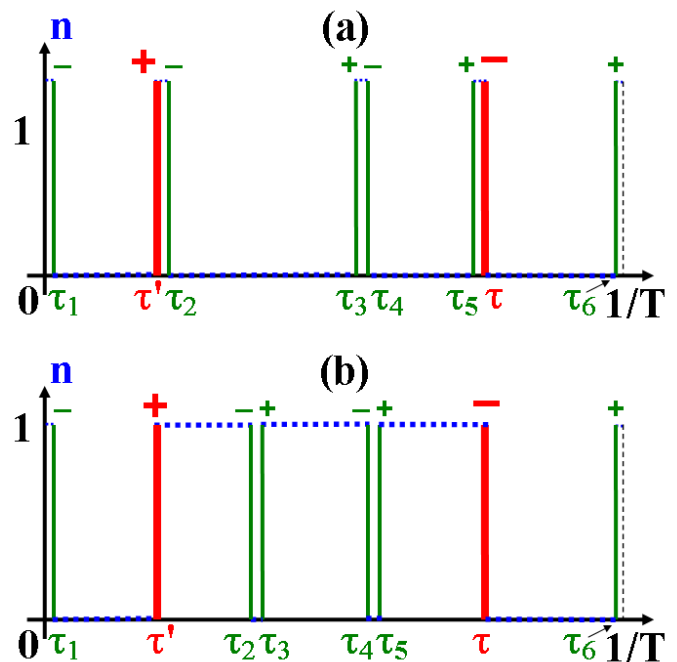


FIG. 2: (Color online) Typical configuration of the CG expansion for the dot Green function [Eqs. (5)–(6); here $\tau > \tau'$, $s = -1$, $2N = 6$, $s' = 1$, $M = 0$, and $2M' = 4$, as in Fig. 1(b)] for (a) large $|\varepsilon_0|$ in both phases (and possibly small $|\varepsilon_0|$ in the weak-coupling phase³⁵) — d-charges are screened; (b) small $|\varepsilon_0|$ in the weak-coupling phase — d-charges are not screened. Notations are the same as in Fig. 1. See the text for further details.

tively decoupled, the usual $|\omega|^{1/g-1}$ behavior at the end of a LL wire need not apply anymore.

One could actually proceed to study higher order terms in the weak-coupling regime (and similarly, for large $|\varepsilon_0|$ in the strong-coupling phase). For small t_0 the leading correction is dressing of the above-mentioned charge configurations by a series of pairs of close-by t_0 -charges (close-by since $|\varepsilon_0|$ and/or α_{FES} are large), as depicted in Fig. 2. One then has to sum over all the terms similar to Fig. 2(a) for large $|\varepsilon_0|$ (i.e., for $|\omega| \ll |\varepsilon_0|$ in the weak-coupling phase) or all the terms similar to Fig. 2(b) for small $|\varepsilon_0|$ (i.e., for $|\omega| \gg |\varepsilon_0|$). Since each pair has a very small dipole moment (due to the proximity of the charges), inter-pair interactions are negligible in a first approximation. This is actually an imaginary time variant of the noninteracting blip approximation (NIBA)^{24,25}. The following argument can spare us the need of explicit calculations. For $U_0 = 0$ and $K = 0$, the d-charges are noninteracting, $\vec{e}_d = (0, 0)$. The sum over all the terms with pairs of nearby t_0 charges would be the same (in the current approximation) as the Green function of a *noninteracting* system consisting of a level tunnel-coupled to a bath of *noninteracting* fermions with power-law local density of states $\rho_L(\omega) \sim |\omega|^{\alpha_{\text{FES}} - 1}$ (with some appropriate high-energy cutoff and normalization). For the latter system the Green function can be easily

evaluated to give $G_D^0(i\omega) = [i\omega - \varepsilon_0 - \Sigma_D^0(i\omega)]^{-1}$, where the dot self energy is³³:

$$\Sigma_D^0(i\omega) = (t_0)^2 \int_{-\infty}^{\infty} \frac{\rho_L(\Omega)}{i\omega - \Omega} d\Omega, \quad (11)$$

so that $\Sigma_D^0(i\omega) \sim \omega^{\alpha_{\text{FES}}-1}$. For small $|\varepsilon_0|$ we indeed see that $\Sigma_D^0(\omega)$ is subdominant with respect to the noninteracting contribution only if $\alpha_{\text{FES}} > 2$, which is exactly the condition for the weak-coupling phase for small t_0 . Then, exactly at $\varepsilon_0 = 0$, a delta-function term appears at $\omega = 0$ in the expression for the LDoS (similarly to the situation at $t_0 = 0$), whose coefficient is determined by the requirement that the integral of the entire expression for the LDoS corresponding to $G_D^0(i\omega)$ is unity¹⁴.

Before discussing nonzero U_0 and K , it should be remarked that this NIBA-like approximation exactly reproduces the perturbative (in the tunneling t_0) approach employed in Ref. 19, and would lead to similar predictions for the behavior of the level population. Both approximations are justified only in the weak-coupling phase (or when $|\varepsilon_0|$ is large), but not in the strong-coupling phase, where t_0 grows under RG flow and thus cannot be treated perturbatively, similarly to the exchange J_{xy} in the equivalent Kondo problem³⁴. In the strong-coupling regime perturbative results predict correctly the dependence of the Kondo temperature on t_0 (again, just like in the Kondo model³⁴) and the qualitative behavior of the LDoS for $1/2 < g < 1$ and $\varepsilon_0 \neq 0$ (at $U_0 = 0$ and $K = 0$), but deviate from our previous conclusions in many other respects. For example, as we discuss below, at nonzero U_0 and K our NIBA calculations indicate that the exponent in the power-law behavior of the LDoS at low energy may depend on these interactions too, in contrast with the situation in the strong-coupling phase, where the corresponding exponent depends only on the LL parameter g , as shown above. Moreover, even for vanishing dot-lead and dot-bath interactions (the case treated in Ref. 19) the NIBA/perturbative expression given above does not agree with our previous analysis of the strong-coupling phase: for (a) $1/2 < g < 1$ and $\varepsilon_0 = 0$ or (b) $g > 1$ and any ε_0 , NIBA would suggest that the LDoS varies as $\sim |\omega|^{1-1/g}$, i.e., with the *opposite* exponent to the one appearing in the density of states at the end of a LL wire. Perturbative results would thus imply that the LDoS may be *enhanced* for $g < 1$ or *suppressed* for $g > 1$, which is clearly at odds with both our previous results and the behavior of density of states at the lead edge. Moreover, integrating the perturbative LDoS leads to the prediction that the level population may have a power-law dependence on ε_0 at the strong-coupling phase (for $1/2 < g < 2/3$)¹⁹, which is in contrast with the analytical behavior expected from the exact mapping of our model onto the Kondo problem, as discussed above. To summarize, NIBA/perturbative (in t_0) expressions do not hold in general in the strong-coupling phase. It may be noted that the numerical data of Ref. 19 does not cover these regimes of the strong coupling phase for which perturba-

tive calculations disagree with our previous analysis.

Returning to the discussion of the NIBA approximation for the weak-coupling phase, we will now treat the more general case, i.e., nonzero U_0 and K (which was not addressed in Ref. 19). Again, screened d-charges terms [Fig. 2(a)] are dominant for $|\omega| \ll |\varepsilon_0|$, whereas unscreened d-charges terms [Fig. 2(b)] are dominant for $|\omega| \gg |\varepsilon_0|$.³⁵ Let us start from the latter case. Now that there is interaction between d-charges, the CG expression for the Green function $G_D(\tau - \tau')$ contains an additional a factor of the form $\sim |\tau - \tau'|^{-\alpha_{\text{FES}}^d}$ (interaction of d-charges with the pairs of close-by t_0 -charges is negligible). Turning to the frequency domain, the LDoS of the unscreened d-charges contribution [Fig. 2(b)] will thus be the convolution of the LDoS $\rho_D^0(\omega)$ associated with $G_D^0(i\omega)$ from the previous paragraph, with a function $\rho_{\text{pair}}(\omega) \sim |\omega|^{\alpha_{\text{FES}}^d-1}$, which is simply the LDoS of a decoupled ($t_0 = 0$) level as discussed above, i.e.,

$$\rho_D(\omega) = 2\text{sgn}(\omega) \int_0^{\omega} \rho_D^0(\omega - \Omega) \rho_{\text{pair}}(\Omega) d\Omega, \quad (12)$$

at $T = 0$. Thus, the $|\omega|^{\alpha_{\text{FES}}^d-1}$ behavior of the decoupled level will survive for vanishing $|\varepsilon_0|$, due to the delta peak in $G_D^0(i\omega)$. This behavior actually applies to the entire $|\omega| \gg |\varepsilon_0|$ region, which is exactly where the contribution of terms similar to Fig. 2(b) is important. Higher order corrections will give extra powers of $|\omega|^{\alpha_{\text{FES}}-2}$, which are subleading since $\alpha_{\text{FES}} > 2$.

Similar considerations apply to the screened d-charges contribution [Fig. 2(a)] when $|\omega| \ll |\varepsilon_0|$. For $U_0 \neq 0$ and/or $K \neq 0$, two corrections are due. The first correction takes into account the factors coming from the interaction between each d-charge and the neighboring t_0 -charge, which are power-laws in the time domain. Since the d- t_0 charges form tightly-bound pairs, we can take the limits of integration over their separation to infinity. They thus yield factors of

$$\int_0^{\infty} \left(\frac{\xi}{\tilde{\tau}}\right)^{\vec{e}_0 \cdot \vec{e}_d} e^{-|\varepsilon_0|\tilde{\tau}} \frac{d\tilde{\tau}}{\xi} = \frac{\Gamma(1 - \vec{e}_0 \cdot \vec{e}_d)}{(|\varepsilon_0|\xi)^{1 - \vec{e}_0 \cdot \vec{e}_d}}, \quad (13)$$

where $\Gamma(z)$ is the gamma function³⁶, and $\vec{e}_0 \cdot \vec{e}_d = (\alpha_{\text{FES}}^d + \alpha_{\text{FES}} - 1/g)/2$. The correction is then the ratio between this expression and its value at $\vec{e}_d = 0$. Apart from this constant factor, one must compensate for the fact that the inter-pair interaction of these two d- t_0 pairs gives the Green function a factor which varies as $|\tau - \tau'|^{-1/g}$ (since $|\vec{e}_d - \vec{e}_0|^2 = 1/g$), instead of the $|\tau - \tau'|^{-\alpha_{\text{FES}}}$ dependence used in the calculation of G_D^0 . Hence, $\rho_D^0(\omega)$ should be convoluted here with $\sim |\omega|^{1/g - \alpha_{\text{FES}} - 1}$. For $|\omega| \ll |\varepsilon_0|$ the LDoS will thus retain the $|\omega|^{1/g-1}$ behavior of the strong-coupling phase.

To conclude the discussion of this NIBA-type approximation, a general expression for the LDoS which interpolates between large and small $|\omega/\varepsilon_0|$ limits³⁵ is of the

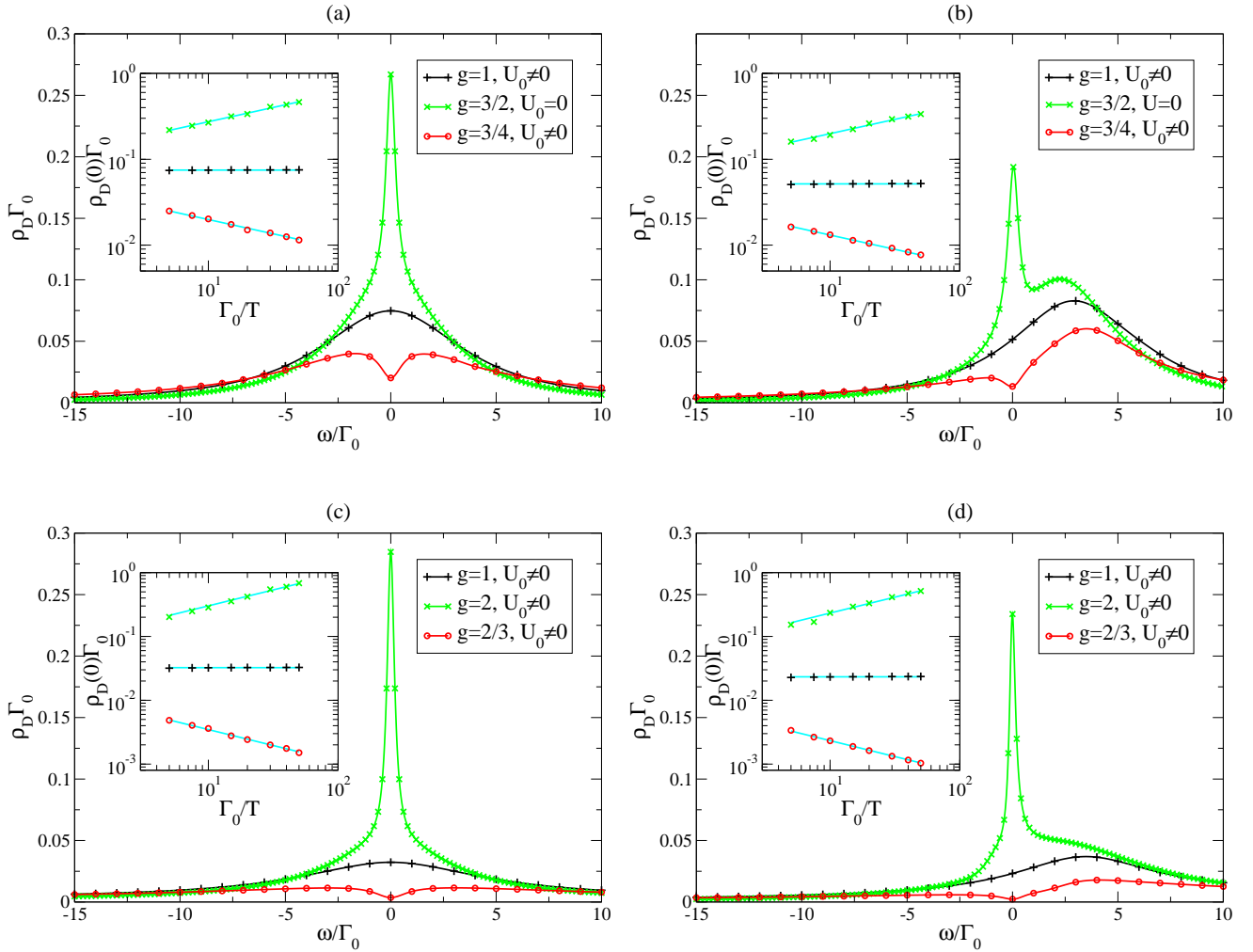


FIG. 3: (Color online) MC results for the LDoS as a function of frequency (measured with respect to the Fermi energy) for three different models, all with $\alpha_{\text{FES}} = 2/3$ and $T/\Gamma_0 = 0.1$. The three curves in each panel correspond to three different values of g : $g = 1$ (black pluses), $g > 1$ (green X's), and $g < 1$ (red circles), as indicated in the legends. The insets present the the LDoS at the Fermi energy as a function of the temperature $\rho_D(0)$ (with the same code as before), together with a cyan line showing best-fit to the expected power-law behavior $\rho_D(0) \sim T^{1/g-1}$ (only the prefactor is fitted). The different panels correspond to different values of ε_0 and K : (a) $\varepsilon_0 = 0$ and $K = 0$; (b) $\varepsilon_0 = 2\Gamma_0$ and $K = 0$; (c) $\varepsilon_0 = 0$ and $K = 1/6$; (d) $\varepsilon_0 = 2\Gamma_0$ and $K = 1/6$. In each case the value of U_0 was chosen according to the requirement $\alpha_{\text{FES}} = 2/3$.

form of Eq. (12), but with $\rho_{\text{pair}}(\Omega)$ replaced by

$$\rho'_{\text{pair}}(\Omega) \sim |\Omega|^{\alpha_{\text{FES}}^d - 1} \left| \frac{\varepsilon_0}{\Omega} - 1 \right|^{\alpha_{\text{FES}} + \alpha_{\text{FES}}^d - 1/g}. \quad (14)$$

All the low-energy results of this section are summarized in Table I.

IV. NUMERICAL CALCULATIONS

In this section we present the results of numerical calculations, verifying the conclusions of our previous analysis, i.e., that the LDoS at low energies features a power-law behavior with the power determined by LL physics only (in the strong coupling phase), although, as we have

shown before²¹, its integral (the level population) is universal, and cannot be used to extract LL parameters.

To calculate the LDoS we used classical Monte-Carlo (MC) simulations on the CG expansion of dot Green function²⁸. The MC update procedure used is similar to the one employed recently for the closely-related continuous time quantum MC algorithm³⁷. After obtaining the imaginary-time Green function it was Fourier-transformed to Matsubara frequencies, followed by analytic continuation to real frequencies using the Padé approximant technique³⁸. This yields the retarded Green function, whose imaginary part is proportional to the LDoS³³. Below we present data in the non-perturbative strong-coupling region, which confirms the results of our previous analysis. Actually, in the weak-coupling phase (which is accessible analytically through the NIBA-like

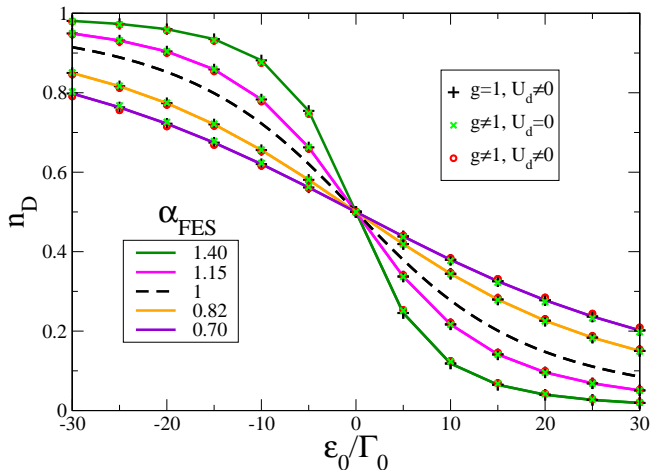


FIG. 4: (Color online) DMRG results for the average level occupancy n_D as a function of its energy, ε_0 , for a discrete model of the lead [Eqs. (15)–(16)]. The curves on which the symbols reside (which serve as guides to the eye) correspond to the various α_{FES} values, where the larger α_{FES} the narrower the curve and vice versa. The widest curve has similar parameters to those used in the MC simulations presented in Fig. 3. On each curve there are three different choices of U and U_d (all giving the same α_{FES} value), denoted by the three different symbol types. See the text for further details.

approximation) MC simulations are not efficient, since there CG charges are rare and averaging very slow. In this sense, our analysis and numerical calculations are complementary.

The results presented in the different panels Fig. 3. The values of g , U_0 and K are varied, in a way which keeps α_{FES} constant at a value of $2/3$. Hence, the occupancies as functions of ε_0 are the same, as we also verify below (actually, the CG representation would predict exactly identical occupations). The LDoS curves are, however, markedly different: depending on whether $g > 1$, $g < 1$, or $g = 1$, they have a maximum, a minimum, or no special feature near the Fermi energy, respectively. In the inset we demonstrate that in all cases the LDoS at the Fermi energy exhibits power-law dependence on temperature, $\rho_D(0) \sim T^{1/g-1}$, as found in the previous section (cf. Table I).

For the sake of completeness, we will repeat here some of our previous data on the level occupancy²¹. Since the MC simulation is based on the CG, to have an independent check of the universality of the level population we employed the density matrix renormalization group (DMRG)³⁹ algorithm, using block-sizes of up to 256. DMRG is also better suited to ground state calculations, and thus complements the necessarily finite-temperature MC in this respect. The model used is a half-filled tight binding chain with nearest-neighbor in-

teractions. It is described by the Hamiltonian:

$$H_L = \sum_{i=1}^{N-1} \left[t c_i^\dagger c_{i+1} + \text{H.c.} + U \left(c_i^\dagger c_i - \frac{1}{2} \right) \left(c_{i+1}^\dagger c_{i+1} - \frac{1}{2} \right) \right] \quad (15)$$

where c_i^\dagger (c_i) is the electronic creation (annihilation) operator at the i th site of the wire ($i = 1 \dots N$, with $L = Na$), and t and U are, respectively, nearest-neighbor hopping amplitude and interaction strength. The low energy physics of this model is known to be governed by LL theory for not too large interactions (i.e., $|U| < 2t$),¹ with $g = \pi/[2 \cos^{-1}(-U/2t)]$ and $v/(2at) = \pi \sqrt{1 - (U/2t)^2}/[2 \cos^{-1}(U/2t)]$. The dot is still governed by the same $H_D = \varepsilon_0 d^\dagger d$, and is coupled to the lead through:

$$H_{DL} = t_d c_1^\dagger d + \text{H.c.} + U_d \left(d^\dagger d - \frac{1}{2} \right) \left(c_1^\dagger c_1 - \frac{1}{2} \right) \quad (16)$$

t_d , U_d are related to the corresponding parameters of the continuum version Eq. (2) by $t_0 = t_d \sqrt{a}$, and $U_0 = U_d a$, a being the lattice spacing. We have previously shown that boundary conformal field theory arguments and the Bethe ansatz solution yield that here $\delta_{\text{eff}} = \tan^{-1}(U_d/\sqrt{4t^2 - U^2})$.²¹

The level population is plotted in Fig. 4 as a function of ε_0 . Different curves correspond to different values of α_{FES} , as indicated in the legend. On each such curve there are three types of symbols, denoting DMRG data on three different models: (i) $g = 1$ (i.e., $U = 0$) but nonzero U_d ; (ii) $g \neq 1$ (nonzero U) but $U_d = 0$; (iii) both U and U_d are nonzero. All the models are without coupling to the bath ($K = 0$). The values of U and U_d in each model were chosen so as to give the same value of α_{FES} for each curve. For model (iii) we used $U = \pm 0.5t$, with sign opposite to that of model (ii). In all cases we chose t_d to get $\Gamma_0 = 10^{-4}t$ and used $N = 100v/(at)$ sites. The results clearly show that the occupancy is indeed universal, depending only on α_{FES} , and not on the strengths or signs of the interactions (U and U_d). It should be noted that the widest curve has similar parameters to those used in the MC simulations (Fig. 3).

V. CONCLUSIONS

To summarize, we have studied, both analytically and numerically, the LDoS of a level coupled to a LL and to an Ohmic bath over the entire parameter space. We have found that in general it exhibits a power-law dependence at low energies. In large parts of the phase space this is just the power-law behavior of the tunneling density of states at the end of a LL wire. Thus, a measurement of the LDoS there can be used to extract the value of the LL interaction parameter g . In other regions it is also affected by level-lead and level-bath interactions. In any case the LDoS is explicitly sensitive to the value of the LL parameter g , although the LDoS determines the level

population, which was found before to be universal²¹, and thus not to feature any LL-specific power-law.

Acknowledgments

We would like to thank Y. Weiss for his invaluable help with the DMRG calculations, A. Schiller for many useful

suggestions, and Y. Gefen for discussions. M.G. is supported by the Adams Foundation of the Israel Academy of Sciences and Humanities. Financial aid from the Israel Science Foundation (Grant 569/07) is gratefully acknowledged.

-
- ¹ A.O. Gogolin, A.A. Nersesyan, and A.M. Tsvelik, *Bosonization and Strongly Correlated Systems*, (Cambridge University Press, Cambridge, 1998); T. Giamarchi, *Quantum Physics in One Dimension*, (Oxford University Press, Oxford, 2003).
 - ² For a review see: A.M. Chang, Rev. Mod. Phys. **75**, 1449 (2003), and references cited therein.
 - ³ For a review see: M. König, H. Buhmann, L.W. Molenkamp, T. Hughes, C.-X. Liu, X.-L. Qi, and S.-C. Zhang, J. Phys. Soc. Jpn. **77**, 031007 (2008), and references cited therein.
 - ⁴ C.L. Kane and M.P.A. Fisher, Phys. Rev. Lett. **68**, 1220 (1992); Phys. Rev. B **46**, R7268 (1992); **46**, 15233 (1992).
 - ⁵ A. Furusaki and N. Nagaosa, Phys. Rev. B **47**, 3827 (1993).
 - ⁶ A. Furusaki, Phys. Rev. B **57**, 7141 (1998).
 - ⁷ O.M. Auslaender, A. Yacoby, R. de Picciotto, K.W. Baldwin, L.N. Pfeiffer, and K.W. West, Phys. Rev. Lett. **84**, 1764 (2000).
 - ⁸ H.W.Ch. Postma, T. Teepen, Z. Yao, M. Grifoni, and C. Dekker, Science **293**, 76 (2001).
 - ⁹ A. Komnik and A.O. Gogolin, Phys. Rev. Lett. **90**, 246403 (2003); Phys. Rev. B **68**, 235323 (2003).
 - ¹⁰ Yu.V. Nazarov and L.I. Glazman, Phys. Rev. Lett. **91**, 126804 (2003).
 - ¹¹ D.G. Polyakov and I.V. Gornyi, Phys. Rev. B **68**, 035421 (2003).
 - ¹² I.V. Lerner, V.I. Yudson, and I.V. Yurkevich, Phys. Rev. Lett. **100**, 256805 (2008).
 - ¹³ M. Goldstein and R. Berkovits, Phys. Rev. Lett. **104**, 106403 (2010).
 - ¹⁴ A. Furusaki and K.A. Matveev, Phys. Rev. Lett. **88**, 226404 (2002).
 - ¹⁵ M. Sade, Y. Weiss, M. Goldstein, and R. Berkovits, Phys. Rev. B **71**, 153301 (2005);
 - ¹⁶ K. Le Hur and M.-R. Li, Phys. Rev. B **72**, 073305 (2005).
 - ¹⁷ Y. Weiss, M. Sade, M. Goldstein, and R. Berkovits, Phys. Stat. Sol. (b) **243**, 399 (2006); Y. Weiss, M. Goldstein, and R. Berkovits, J. Phys.: Condens. Matter **19**, 086215 (2007);
 - ¹⁸ Y. Weiss, M. Goldstein, and R. Berkovits, Phys. Rev. B **75**, 064209 (2007); **76**, 024204 (2007); **77**, 205128 (2008).
 - ¹⁹ P. Wächter, V. Meden, and K. Schönhammer, Phys. Rev. B **76**, 125316 (2007).
 - ²⁰ G.A. Fiete, W. Bishara, C. Nayak, Phys. Rev. Lett. **101**, 176801 (2008); Phys. Rev. B **82**, 035301 (2010).
 - ²¹ M. Goldstein, Y. Weiss, and R. Berkovits, Europhys. Lett. **86**, 67012 (2009); Proceedings of FQMT '08, Physica E **42**, 610 (2010).
 - ²² F. Elste, D.R. Reichman, and A.J. Millis, Phys. Rev. B **81**, 205413 (2010).
 - ²³ A non-chiral LL with a boundary can mapped onto a chiral LL by unfolding the decoupled (Bogolubov-transformed) right- and left-movers [M. Fabrizio and A.O. Gogolin, Phys. Rev. B **51**, 17827 (1995)].
 - ²⁴ A.J. Leggett, S. Chakravarty, A.T. Dorsey, M.P.A. Fisher, A. Garg, and W. Zwerger, Rev. Mod. Phys. **59**, 1 (1987).
 - ²⁵ U. Weiss, *Quantum Dissipative Systems* (World Scientific, Singapore, 1999).
 - ²⁶ A. Kamenev and Y. Gefen, Phys. Rev. B **54**, 5428 (1996); arXiv:cond-mat/9708109.
 - ²⁷ P.W. Anderson and G. Yuval, Phys. Rev. Lett. **23**, 89 (1969); G. Yuval and P.W. Anderson, Phys. Rev. B **1**, 1522 (1970); P.W. Anderson, G. Yuval, and D.R. Hamann, *ibid.* **1**, 4464 (1970).
 - ²⁸ K.D. Schotte and U. Schotte, Phys. Rev. B **4**, 2228 (1971).
 - ²⁹ P.B. Wiegmann and A.M. Finkelstein, Zh. Eksp. Teor. Fiz. **75**, 204 (1978) [Sov. Phys. JETP **48**, 102 (1978)].
 - ³⁰ Q. Si, and G. Kotliar, Phys. Rev. B **48**, 13881 (1993).
 - ³¹ M. Fabrizio, A.O. Gogolin, and P. Nozières, Phys. Rev. B **51**, 16088 (1995).
 - ³² P. Nozières and C.T. De Dominicis, Phys. Rev. **178**, 1097 (1969).
 - ³³ G.D. Mahan, *Many-Particle Physics* (Kluwer, New York, 2000).
 - ³⁴ A.C. Hewson, *The Kondo Problem to Heavy Fermions* (Cambridge University Press, Cambridge, 1993).
 - ³⁵ When $1/g < \alpha_{\text{FES}}^d$ (i.e., in the presence of strong dot-lead and/or dot-bath interactions), interaction between d-charges is large enough to make the screened d-charges contribution [Fig. 2(a)] dominant even for small $|\varepsilon_0|$. Using similar methods one can show that then the LDoS will vary as $|\omega|^{1/g-1}$, just like for $|\omega| \ll |\varepsilon_0|$.
 - ³⁶ M. Abramowitz and I.A. Stegun, *Handbook of Mathematical Functions* (Dover, New York, 1964).
 - ³⁷ P. Werner, A. Comanac, L. de' Medici, M. Troyer, and A.J. Millis, Phys. Rev. Lett. **97**, 076405 (2006); P. Werner and A.J. Millis, Phys. Rev. B **74**, 155107 (2006).
 - ³⁸ H.J. Vidberg and J.W. Serene, J. Low Temp. Phys. **29**, 179 (1977).
 - ³⁹ U. Schollwöck, Rev. Mod. Phys. **77**, 259 (2005); K.A. Hallberg, Adv. Phys. **55**, 477 (2006).